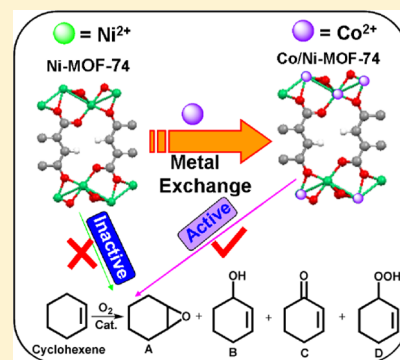


Mixed-Metal Strategy on Metal–Organic Frameworks (MOFs) for Functionalities Expansion: Co Substitution Induces Aerobic Oxidation of Cyclohexene over Inactive Ni-MOF-74

Dengrong Sun, Fangxiang Sun, Xiaoyu Deng, and Zhaohui Li*

Research Institute of Photocatalysis, State Key Laboratory of Photocatalysis on Energy and Environment, Fuzhou University, Fuzhou, 350002, People's Republic of China

ABSTRACT: Different amounts of Co-substituted Ni-MOF-74 have been prepared via a post-synthetic metal exchange. Inductively coupled plasma mass spectrometry, powder X-ray diffraction (XRD), N_2 adsorption/desorption, and extended X-ray absorption fine structure (EXAFS) analyses indicated the successful metathesis between Co and Ni in Ni-MOF-74 to form the solid-solution-like mixed-metal Co/Ni-MOF-74. It was found that introduction of active Co into the Ni-MOF-74 framework enabled the inert Ni-MOF-74 to show activity for cyclohexene oxidation. Since Co was favorably substituted at positions more accessible to the substrate, the mixed-metal Co/Ni-MOF-74 showed superior catalytic performance, compared with pure Co-MOF-74 containing a similar amount of Co. This study provides a facile method to develop solid-solution-like MOFs for heterogeneous catalysis and highlights the great potential of this mixed-metal strategy in the development of MOFs with specific endowed functionalities.



INTRODUCTION

Metal–organic frameworks (MOFs) are a class of crystalline microporous hybrid materials constructed from metal or metal clusters interconnected by organic linkers.¹ Their inherent high specific surface areas, and uniform but tunable cavities, make them to show potentials in a variety of applications.² The structural complexity of MOFs and their adjustable characters, because of the versatile coordination chemistry of the metal cations and the availability of different organic linkers, enable MOFs to be an appealing platform to integrate different functional building blocks into one MOF framework for multifunctional applications. The recently developed mixed-metal approach over MOFs allows for incorporation of two different metals into a same framework to form solid-solution-like mixed-metal MOFs,³ which offers MOFs with an additional degree of structural complexity and is expected to endow them with new functionalities, since their properties are dependent on the incorporated metal atoms. Actually, some pioneering studies have already shown that the mixed-metal MOFs did exhibit properties superior to their parent MOFs and, in some cases, can even induce new functionalities, because of the introduction of the second metal ions. For example, Hill and co-workers have reported that substitution of Zr with Ti in NH_2 -Uio-66(Zr) can improve its adsorption capacity toward CO_2 .⁴ Our previous work showed that the Ti moiety in the mixed-metal NH_2 -Uio-66(Zr/Ti) can act as an electron mediator to facilitate the linker-to-metal charge transfer, which resulted in improved photocatalytic performance.⁵ The introduction of reduced-metal cations such as Ti^{3+} and Fe^{2+} into MOF-5 framework enabled redox reactivity to inert MOF-5.⁶ These results suggest that the

mixed-metal approach on MOFs provides great opportunities to obtain MOFs with specific functionalities. However, studies on the mixed-metal effect on the properties of these solid-solution-like MOFs remained largely unexplored, especially on the field of heterogeneous catalysis, which is believed to be one of the most promising applications of MOF materials.

M-MOF-74 is a three-dimensional honeycomb-like network constructed from divalent metal ions coordinated to 2,5-dihydroxyterephthalic acid (H_4DOBD C).⁷ Our previous work has shown that Co-MOF-74 is active for cyclohexene oxidation while the isostructural Ni-MOF-74 is inactive for this reaction.⁸ Herein, we reported that the substitution of Ni^{2+} in Ni-MOF-74 framework by active Co^{2+} via a post-synthetic metal exchange method can enable the inert Ni-MOF-74 to show catalytic activity for cyclohexene oxidation. The performance over the Co-substituted Ni-MOF-74 (Co/Ni-MOF-74) increased with the amount of incorporated Co^{2+} , indicating that the incorporated Co^{2+} is responsible for the reaction. It is interesting to determine that the mixed-metal Co/Ni-MOF-74 showed superior catalytic performance, compared with pure Co-MOF-74 containing a similar amount of Co^{2+} , because Co^{2+} was favorably substituted at positions more accessible to the substrates.

EXPERIMENTAL SECTION

Materials. 2,5-Dihydroxyterephthalic acid (H_4DOBD C) was obtained from Alfa Aesar Co. Cyclohexene (GR, Aladdin Reagent Co), cobaltous nitrate ($Co(NO_3)_2 \cdot 6H_2O$), nickel nitrate ($Ni(NO_3)_2 \cdot$

Received: June 6, 2015

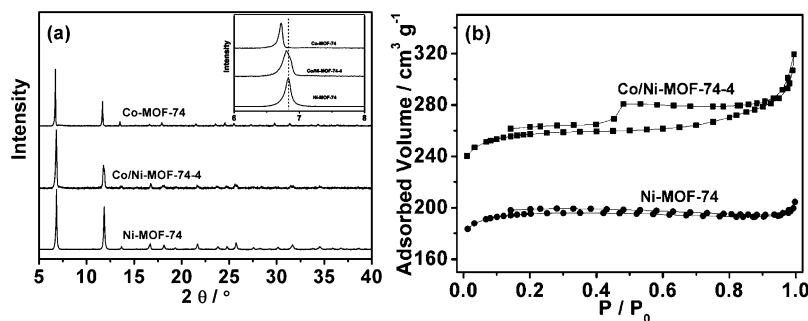


Figure 1. (a) XRD patterns of the as-prepared Ni-MOF-74, Co/Ni-MOF-74-4, and Co-MOF-74 (inset shows enlarged regions of the XRD patterns); (b) N_2 adsorption/desorption isotherms of prepared Ni-MOF-74 and Co/Ni-MOF-74-4 (77 K).

$6\text{H}_2\text{O}$), dimethylformamide (DMF), and ethanol (EtOH) were all used without further purification.

Synthesis of Ni-MOF-74 and Co-MOF-74. Ni-MOF-74 was prepared following the previous reported procedures.⁸ A solid mixture of H_4DOBDC (0.2216 g, 1.12 mmol) and $\text{Ni}(\text{NO}_3)_2 \cdot 6\text{H}_2\text{O}$ (1.077 g, 3.70 mmol) were added to a 75 mL solution of DMF, EtOH and H_2O in 1:1:1 ratio. The above mixture was stirred at room temperature to get a homogeneous solution and was transferred into a 100 mL Teflon liner and heated at 120 °C for 24 h. After reaction, the solids were separated from the solvent via centrifugation, and then washed with fresh DMF and methanol. After that, the sample was treated under vacuum at 180 °C for 5 h to obtain the final Ni-MOF-74. A similar procedure was applied in the preparation of Co-MOF-74, except that $\text{Ni}(\text{NO}_3)_2 \cdot 6\text{H}_2\text{O}$ was replaced with $\text{Co}(\text{NO}_3)_2 \cdot 6\text{H}_2\text{O}$.

Synthesis of Co/Ni-MOF-74. $\text{Co}(\text{NO}_3)_2 \cdot 6\text{H}_2\text{O}$ (0.118 g) was dissolved in DMF (5 mL). Ni-MOF-74 (0.1 g) was dispersed in the above solution and stirred for 30 min. After that, the obtained suspension was sealed and incubated at 80 °C for different times to obtain different amounts of Co-substituted Ni-MOF-74. After reaction, the solids were separated from the solvent via centrifugation, washed with fresh DMF and methanol, extracted by Soxhlet extractor with deionized water overnight, and dried to obtain Co/Ni-MOF-74.

Characterizations. X-ray diffraction (XRD) patterns were collected on a Model D8 Avance X-ray diffractometer (Bruker, Germany) with $\text{Cu K}\alpha$ radiation. Ultraviolet–visible (UV–vis) diffuse reflectance spectra (UV–DRS) of the powders were obtained for the dry-pressed disk samples using a Cary 500 Scan Spectrophotometer (Varian, USA). BaSO_4 was used as a reflectance standard in the UV–DRS experiment. Brunauer–Emmett–Teller (BET) surface area analyses were carried out on a Model ASAP2020 M apparatus (Micromeritics Instrument Corp., USA). For BET surface area analyses, the samples were degassed under vacuum at 200 °C for 6 h and then measured at 77 K. Inductively coupled plasma mass spectrometry (ICP–MS) analysis was performed on a XSERIES 2 system (ThermoFisher). Before the ICP–MS experiment, the solid sample was digested in a mixture of HNO_3 and Milli-Q water (Millipore Corp., Bedford, MA) and the exchanged-out Ni moiety in the solution was collected from the first residual solution. X-ray absorption fine structure (XAFS) spectra were collected in Shanghai Synchrotron Radiation Facility (SSRF) with a Si(111) double-crystal monochromator in transmission mode. The source of BL14W1 is a 38-pole wiggler device with a maximum magnetic field of 1.2 T and a magnet period of 80 mm. The storage ring was operated at 3.5 GeV with injection currents of 100 mA.

Catalytic Reaction. The oxidation of cyclohexene was carried out in a glass reactor that was equipped with a reflux condenser and an oxygen balloon. In a typical reaction, the catalyst (20 mg, 0.4 mmol) and cyclohexene (2 mL, 19.7 mmol) were heated at 80 °C in O_2 under atmospheric pressure. The products were analyzed on a Shimadzu gas chromatograph that was equipped with a flame ionization detection (FID) device and a RTX-5 capillary column. Cyclohexene hydroperoxide was treated with triphenylphosphine (PPh_3) prior to the analyses.

RESULTS AND DISCUSSION

Ni-MOF-74 was prepared following the procedures reported previously.⁸ The similar XRD patterns and comparable Langmuir specific surface area ($860 \text{ m}^2 \text{ g}^{-1}$) of the as-prepared Ni-MOF-74, compared with that previously reported, indicated that Ni-MOF-74 with high quality has been obtained (Figure 1).⁹ Co-substituted Ni-MOF-74 (denoted as Co/Ni-MOF-74- x , where x represents the incubation time) was prepared by exposing Ni-MOF-74 to a DMF solution containing $\text{Co}(\text{NO}_3)_2 \cdot 6\text{H}_2\text{O}$ for different times. The exchange process proceeded slowly at room temperature, but the rate accelerated when the temperature was increased to 80 °C, as evidenced from a gradual color change of the solid from yellow-green to brown (Figure 2, inset). In the meantime, the pink solution

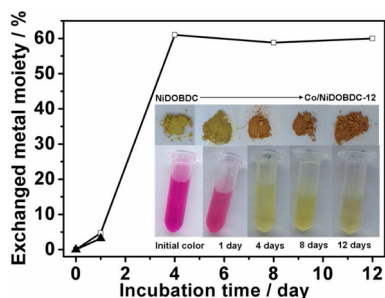


Figure 2. (□) Amount of Co in Ni-MOF-74 and (▲) amount of Ni in the solution determined by ICP–MS analyses after incubation for different times; inset shows photographs of the solid and solution after exchanging for different times. The reaction was carried out in DMF at 80 °C for different times.

gradually faded with the reaction time, suggesting a metathesis between the Co^{2+} cations in solution and the Ni^{2+} cations in the MOF framework. ICP–MS analyses indicated that there was $\sim 4.7\%$ of Co in the solid after 1 day incubation, while a comparable amount of Ni (3.7%) was detected in the resultant solution, which was confirmation that part of the Ni^{2+} cations in Ni-MOF-74 had been substituted by Co^{2+} cations in the solution (Figure 2). The exchange degree can be improved by appropriately extending the incubation time. The amount of Co substituted in the solid increased with the incubation time and reached saturation with ca. 61% of Co incorporated after 4 days of reaction. A prolonged reaction time (8 and 12 days) resulted in only a slightly fluctuated incorporated amount of Co (59% in Co/Ni-MOF-74-8 and 60% for Co/Ni-MOF-74-12). This indicated that not all of the Ni^{2+} cations in Ni-MOF-74 can be replaced by Co^{2+} cations, probably because of the presence of

diffusional limitations in the honeycomb-like network of Ni-MOF-74, which restricts the access of Co^{2+} cations in solution to Ni^{2+} cations in the framework. The good agreement between the XRD patterns of Co/Ni-MOF-74-4 and Ni-MOF-74 suggested that the framework of Ni-MOF-74 was retained after the metalation process (Figure 1a). However, the peak with 2θ value at $\sim 6.8^\circ$ observed over Ni-MOF-74 shifted to lower value after Co incorporation (Figure 1a, inset). Such a shift is probably due to the substitution of smaller Ni^{2+} (0.690 Å) by larger Co^{2+} (0.745 Å), which leads to the expanding of the crystal lattice.¹⁰ The absence of amorphous impurity in the pores was confirmed by the nitrogen adsorption–desorption measurement performed at 77 K (Figure 1b). Similar with Ni-MOF-74, Co/Ni-MOF-74-4 also exhibited a Type I N_2 isotherm with a high Langmuir specific surface area of $1085 \text{ m}^2 \text{ g}^{-1}$. These observations clearly suggested that the incorporated Co^{2+} cations has successfully replaced Ni^{2+} cations in the framework of Ni-MOF-74, instead of residing in the pores. Since the atomic weight of Co (58.9 g mol^{-1}) is comparable to that of Ni (58.7 g mol^{-1}), the higher specific surface area of Co/Ni-MOF-74-4 is probably due to the larger size of Co^{2+} , compared with Ni^{2+} .^{11,12} Actually, a similar improvement in the specific surface area was also reported over Co-substituted Zn-MOF-74, which showed $\sim 32\%$ higher Langmuir specific surface area than pure Zn-MOF-74.¹² The successful substitution of Ni by Co was also supported by extended X-ray absorption fine structure (EXAFS) analyses (see Figure 3, and Table 1). The k^3 -weighted Fourier

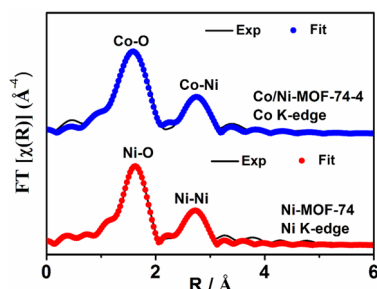


Figure 3. Comparison of the k^3 -weighted Fourier transforms between the Ni K-edge of Ni-MOF-74 and Co K-edge of Co/Ni-MOF-74-4.

Table 1. EXAFS Fit Parameters for the Ni-MOF-74 and Co/Ni-MOF-74-4

path	coordination number, CN	bond length, R (Å)	Debye–Waller factor, σ^2 (Å ²)	goodness-of-fit index, R_{factor} (%)
Fit of Pristine Ni-MOF-74 (<i>K</i> Range = 3.74–12.51, <i>R</i> Range = 0.88–3.12)				
Ni–O	5.59	2.04	0.0060	0.09
Ni–Ni	2.40	3.02	0.0082	
Fit of Co/Ni-MOF-74-4 (<i>K</i> Range = 3.79–10.32, <i>R</i> Range = 1.00–3.22)				
Co–O	6.61	2.04	0.0096	0.41
Co–Ni	2.16	3.04	0.0090	

transforms of the Ni K-edge EXAFS spectrum of Ni-MOF-74 revealed that Ni in Ni-MOF-74 was six-coordinated by O with an average Ni–O bonds of 2.04 Å, in agreement with that in the previous report.⁷ A similar 6-fold coordination environment around Co was also observed in Co/Ni-MOF-74-4, with an average Co–O bond length of 2.04 Å, which is a reasonable value. These indicated that Co has been successfully substituted into the Ni-MOF-74 framework. A lack of observation of peaks

corresponding to other Co species excluded the presence of adsorbed Co or Co-based impurities. These results suggested that Co/Ni-MOF-74 with different amounts of Co incorporated can be facilely obtained via a post-synthetic metal exchange under mild conditions.

Our previous study has revealed that the cycling of Co between Co^{2+} and Co^{3+} is essential for the oxidation of cyclohexene over Co-MOF-74, while the difficulty to form Ni^{3+} in Ni-MOF-74 makes it inert for this reaction.⁸ To study the effect of substituted Co^{2+} in the mixed Co/Ni-MOF-74 for this reaction, the catalytic performance of the as-prepared Co/Ni-MOF-74 for cyclohexene oxidation was investigated. As shown in Table 2 (entries 1 and 2), although Ni-MOF-74 is inactive for cyclohexene oxidation, because of the auto-oxidization of cyclohexene, $\sim 37.2\%$ of cyclohexene was converted over Ni-MOF-74 after reacting for 20 h. This value is comparable to that observed in the system without any catalyst (37.0%). The detectable products from the auto-oxidization of cyclohexene are cyclohexene oxide (A), 2-cyclohexen-1-ol (B), 2-cyclohexen-1-one (C), and cyclohexene hydroperoxide (D); among them, D, as the main product, had a yield of 18.7%. When Co/Ni-MOF-74-1 (with 4.7% Co) was used as the catalyst, although the conversion of the cyclohexene only increased slightly from the original 37.0% to 39.2%, the products distribution changed significantly (Table 2, entry 3). The yield to D decreased from 18.7% over Ni-MOF-74 to 6.6% over Co/Ni-MOF-74-1, with a concomitant increase of the yield to B and C from the original 6.5% and 8.3% to 9.9% and 20.8%, respectively. These observations suggest that the incorporation of Co^{2+} in the framework facilitates the catalytic transformation of D to B and C. The catalytic performance can be enhanced by increasing the amount of Co incorporated in the Ni-MOF-74 framework. For Co/Ni-MOF-74-4, in which 61% of Co^{2+} was incorporated, the conversion of cyclohexene reached 54.7% under similar conditions and almost all D has been converted to B (20.7%) and C (30.4%), showing a high total selectivity of 93.4% to B and C (Table 2, entry 4). After reacting for 20h, Co/Ni-MOF-74-4 was removed from the reaction system and the reaction continued for another 5 h. It was found that the conversion of the cyclohexene only slightly increased from 54.7% to 55.7%, and most of the converted cyclohexene has been transformed to product D (Table 2, entry 5). This phenomenon is similar to that observed in the system without catalyst, indicating the heterogeneous nature of cyclohexene oxidation over Co/Ni-MOF-74-4. Co/Ni-MOF-74-4 is also stable during the catalytic reaction, as confirmed from the similar XRD patterns between the fresh and used Co/Ni-MOF-74-4 (Figure 4). The cycling results also showed that there was no obvious loss of the catalytic activity over Co/Ni-MOF-74-4 after three reaction runs, which is more evidence that the structure of the catalyst was well preserved during the reaction (Figure 5).

The above observations clearly suggest a strong correlation between the catalytic activity and the incorporated Co, which indicates the important role of the substituted Co^{2+} in Co/Ni-MOF-74 for the oxidation of cyclohexene. It is generally known that paramagnetic O_2 is favorable for the reaction with paramagnetic metal ion and the activation of O_2 by Co-containing homogeneous complexes has been well-documented.¹³ Similar to that in homogeneous Co-containing complexes, O_2 can also bind to the Co^{2+} sites in Co/Ni-MOF-74 to form O_2 adduct due to the presence of open metal sites in the MOF framework. Such $\text{Co}-\text{O}_2$ adduct can react with

Table 2. Aerobic Oxidation of Cyclohexene under Different Conditions^a

					Yield (%)			
entry	catalyst	incorporated amount of Co (%)	conversion (%)		A	B	C	D
1	Ni-MOF-74	0	37.0		3.5	6.5	8.3	18.7
2			37.2		3.5	6.5	8.4	18.8
3	Co/Ni-MOF-74-1	4.7	39.2		1.9	9.9	20.8	6.6
4	Co/Ni-MOF-74-4	61.0	54.7		3.0	20.7	30.4	0.6
5 ^b			55.7		3.2	21.0	30.0	1.5

^aReaction conditions: 20 mg of catalyst, 2 mL cyclohexene, O₂ balloon, 80 °C. ^bAfter Co/Ni-MOF-74-4 was removed, the filtrate continued reacting for another 5 h.

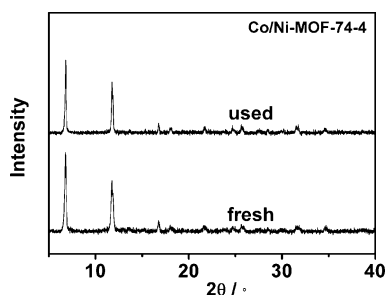


Figure 4. XRD patterns of Co/Ni-MOF-74-4 before and after aerobic cyclohexene oxidation.

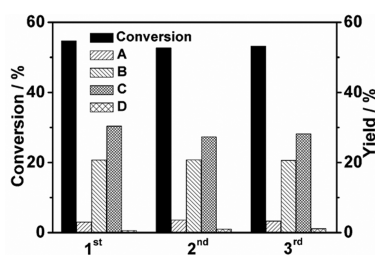


Figure 5. Cycling test on Co/MOF-74-4 for the oxidation of cyclohexene.

cyclohexene to give the hydroperoxo complex ($\text{Co}^{3+}\text{--OOH}$), accompanied by the formation of cyclohexenyl radicals. The fission of Co--O bond in $\text{Co}^{3+}\text{--OOH}$ would recover the Co/Ni-MOF-74 and liberate the peroxy radical (HOO^\bullet), which can react with the cyclohexenyl radicals to give the intermediate D or react with the double bond to give A. Since allylic oxidation of cyclohexene is much easier than its epoxidation, the formation of D was observed as the main reaction, while oxidation of cyclohexene to give A was a minor reaction in the above-mentioned catalytic systems. The as-formed D can be further transformed to form B and C via the Haber–Weiss process involving the cycling of Co between Co^{2+} and Co^{3+} ,^{8,14} which was consistent with the observation that the yield to B

and C improved with the incorporated Co amount in Co/Ni-MOF-74.

Although the role played by the substituted Co^{2+} in Co/Ni-MOF-74 is similar to those in pure Co-MOF-74 reported in our previous work,⁸ it is interesting to find that Co/Ni-MOF-74 exhibited higher catalytic performance for the oxidation of cyclohexene than pure Co-MOF-74 which contains similar amount of Co. As shown in Table 3, the conversion of cyclohexene in 20 h over Co-MOF-74 was 50.0%, among which 15.4% was converted to B and 26.3% was converted to C, showing a total selectivity of 83.4% to B and C. However, the reaction performed over Co/Ni-MOF-74-12 with an equal amount of Co showed a higher conversion of cyclohexene (54.2%) and almost all the product D has been converted to B (20.4%) and C (30.1%) with a total selectivity of 93.2% to B and C under similar condition. Since Co/Ni-MOF-74 and Co-MOF-74 is isostructural and comparable amount of Co was used in these two catalytic systems, it is believed that, in addition to the amount of Co, other factors related to the substituted Co are responsible for their different catalytic performance. The observation that only part of Ni^{2+} in Ni-MOF-74 can be substituted by Co^{2+} implied that the positions where the metathesis occurs are more accessible to the substrate than those unsubstituted sites. Therefore, the substituted Co^{2+} in Co/Ni-MOF-74 is more effective than the overall Co^{2+} in pure Co-MOF-74, leading to a higher catalytic performance of Co/Ni-MOF-74, compared with pure Co-MOF-74 containing a similar amount of Co.

CONCLUSIONS

In summary, partial substitution of Ni^{2+} by Co^{2+} via a post-synthetic metal exchange enabled the inert Ni-MOF-74 to show catalytic activity for cyclohexene oxidation. The mixed-metal Co/Ni-MOF-74 showed superior catalytic performance, compared with pure Co-MOF-74 containing a similar amount of Co^{2+} , because Co^{2+} was favorably substituted at positions more accessible to the substrates. This study provides a facile method to develop solid-solution-like MOFs for heterogeneous

Table 3. Comparison of the Catalytic Performance for Cyclohexene Oxidation between Co-MOF-74 and Co/Ni-MOF-74-12

catalyst	amount of catalyst used (mg)	conversion (%)	Yield (%)			
			A	B	C	D
Co-MOF-74	12	50.0	3.7	15.4	26.3	4.6
Co/Ni-MOF-74-12 (60% of Co incorporated)	20	54.2	3.0	20.4	30.1	0.7

catalysis and highlights the great potential of this mixed-metal strategy in the development of MOFs with specific endowed functionalities.

AUTHOR INFORMATION

Corresponding Author

*E-mail: zhaohuili1969@yahoo.com.

Notes

The authors declare no competing financial interest.

ACKNOWLEDGMENTS

We are grateful to the Shanghai Synchrotron Radiation Facility (SSRF) of China for the XAFS spectra measurements at the BL14W1 beamline. This work was supported by the 973 Program (No. 2014CB239303), the NSFC (No. 21273035), the Specialized Research Fund for the Doctoral Program of Higher Education (No. 20123514110002), and the Independent Research Project of State Key Laboratory of Photocatalysis on Energy and Environment (No. 2014A03). Z.L. thanks the Award Program for Minjiang Scholar Professorship for financial support.

REFERENCES

- (1) (a) Corma, A.; Garcia, H.; LLabres i Xamena, F. X. *Chem. Rev.* **2010**, *110*, 4606–4655. (b) Férey, G. *Chem. Soc. Rev.* **2008**, *37*, 191–214. (c) Férey, G.; Serre, C.; Devic, T.; Maurin, G.; Jobic, H.; Llewellyn, P. L.; De Weireld, G.; Vimont, A.; Daturi, M.; Chang, J.-S. *Chem. Soc. Rev.* **2011**, *40*, 550–562.
- (2) (a) Dhakshinamoorthy, A.; Asiri, A. M.; Garcia, H. *Chem. Soc. Rev.* **2015**, *44*, 1922–1947. (b) Li, J. R.; Sculley, J.; Zhou, H. C. *Chem. Rev.* **2012**, *112*, 869–932. (c) Murray, L. J.; Dincă, M.; Long, J. R. *Chem. Soc. Rev.* **2009**, *38*, 1294–1314. (d) Zhang, T.; Lin, W. *Chem. Soc. Rev.* **2014**, *43*, 5982–5993. (e) Gao, W.-Y.; Chrzanowski, M.; Ma, S. *Chem. Soc. Rev.* **2014**, *43*, 5841–5866. (f) Fu, Y.; Sun, D.; Chen, Y.; Huang, R.; Ding, Z.; Fu, X.; Li, Z. *Angew. Chem., Int. Ed.* **2012**, *51*, 3364–3367. (g) Rowsell, J. L. C.; Yaghi, O. M. *Angew. Chem., Int. Ed.* **2005**, *44*, 4670–4679. (h) Chen, Y.; Hoang, T.; Ma, S. *Inorg. Chem.* **2012**, *51*, 12600–12602. (i) Chen, Y.-Z.; Xu, Q.; Yu, S.-H.; Jiang, H.-L. *Small* **2015**, *11*, 71–76. (j) Zhang, W.; Lu, G.; Cui, C.; Liu, Y.; Li, S.; Yan, W.; Xing, C.; Chi, Y. R.; Yang, Y.; Huo, F. *Adv. Mater.* **2014**, *26*, 4056–4060. (k) Feng, D.; Jiang, H.-L.; Chen, Y.-P.; Gu, Z.-Y.; Wei, Z.; Zhou, H.-C. *Inorg. Chem.* **2013**, *52*, 12661–12667.
- (3) (a) Kim, M.; Cahill, J. F.; Fei, H.; Prather, K. A.; Cohen, S. M. *J. Am. Chem. Soc.* **2012**, *134*, 18082–18088. (b) Wang, L. J.; Deng, H.; Furukawa, H.; Gandara, F.; Cordova, K. E.; Peri, D.; Yaghi, O. M. *Inorg. Chem.* **2014**, *53*, 5881–5883. (c) Kim, M.; Cahill, J. F.; Su, Y.; Prather, K. A.; Cohen, S. M. *Chem. Sci.* **2012**, *3*, 126–130. (d) Das, S.; Kim, H.; Kim, K. *J. Am. Chem. Soc.* **2009**, *131*, 3814–3815. (e) Brozek, C. K.; Dincă, M. *Chem. Sci.* **2012**, *3*, 2110–2113. (f) Fei, H.; Cahill, J. F.; Prather, K. A.; Cohen, S. M. *Inorg. Chem.* **2013**, *52*, 4011–4016. (g) Fu, H.-R.; Xu, Z.-X.; Zhang, J. *Chem. Mater.* **2015**, *27*, 205–210. (h) Yang, H.; He, X.-W.; Wang, F.; Kang, Y.; Zhang, J. *J. Mater. Chem.* **2012**, *22*, 21849–21851. (i) He, Y.-P.; Tan, Y.-X.; Zhang, J. *J. Mater. Chem. C* **2014**, *2*, 4436–4441.
- (4) Lau, C. H.; Babarao, R.; Hill, M. R. *Chem. Commun.* **2013**, *49*, 3634–3636.
- (5) Sun, D.; Liu, W.; Qiu, M.; Zhang, Y.; Li, Z. *Chem. Commun.* **2015**, *51*, 2056–2059.
- (6) Brozek, C. K.; Dincă, M. *J. Am. Chem. Soc.* **2013**, *135*, 12886–12891.
- (7) Dietzel, P. D. C.; Panella, B.; Hirscher, M.; Blom, R.; Fjellvåg, H. *Chem. Commun.* **2006**, 959–961.
- (8) Fu, Y.; Sun, D.; Qin, M.; Huang, R.; Li, Z. *RSC Adv.* **2012**, *2*, 3309–3314.
- (9) Ruano, D.; Díaz-García, M.; Alfayate, A.; Sánchez-Sánchez, M. *ChemCatChem* **2015**, *7*, 674–681.
- (10) Shannon, R. D. *Acta Crystallogr., Sect. A: Cryst. Phys., Diffraction, Theor. Gen. Crystallogr.* **1976**, *A32*, 751–767.
- (11) Caskey, S. R.; Wong-Foy, A. G.; Matzger, A. J. *J. Am. Chem. Soc.* **2008**, *130*, 10870–10871.
- (12) Botas, J. A.; Calleja, G.; Sánchez-Sánchez, M.; Orcajo, M. G. *Int. J. Hydrogen Energy* **2011**, *36*, 10834–10844.
- (13) Henrici-Olivé, G.; Olivé, S. *Angew. Chem., Int. Ed. Engl.* **1974**, *13*, 29–38.
- (14) Hamilton, D. E.; Drago, R. S.; Zombeck, A. *J. Am. Chem. Soc.* **1987**, *109*, 374–379.